Structure and Interactions in Perfluorooctanoate Micellar Solutions Revealed by Small-Angle Neutron Scattering and Molecular Dynamics Simulations Studies: Effect of Urea

Samhitha Kancharla,[1] Dengpan Dong,[2] Dmitry Bedrov,[2*] Marina Tsianou,[1*] Paschalis Alexandridis[1*]

[1] Department of Chemical and Biological Engineering, University at Buffalo, The State University of New York (SUNY), Buffalo, NY 14260-4200, USA

[2] Department of Materials Science and Engineering, University of Utah, 122 S. Central Campus Drive, Room 304, Salt Lake City, UT 84112, USA

* Corresponding Authors:

Paschalis Alexandridis <palexand@buffalo.edu>, Marina Tsianou <mtsianou@buffalo.edu>, and Dmitry Bedrov <d.bedrov@utah.edu>

ABSTRACT

The self-assembly of surfactants in aqueous solution can be modulated by the presence of additives including urea, which is a well-known protein denaturant and also present in physiological fluids and agricultural run-off. This study addresses the effects of urea on the structure of micelles formed in water by the fluorinated surfactant perfluoro-n-octanoic acid ammonium salt (PFOA). Analysis of small-angle neutron scattering (SANS) experiments and atomistic molecular dynamics (MD) simulations provide consensus strong evidence for the direct mechanism of urea action on micellization: urea helps solvate the hydrophobic micelle core by localizing at the surface of the core in the place of some water molecules. Consequently, urea decreases electrostatic interactions at the micelle shell, changes the micelle shape from prolate ellipsoid to sphere, and decreases the number of surfactant molecules associating in a micelle. These findings inform the interactions and behavior of surface active per- and polyfluoroalkyl substances (PFAS) released in the aqueous environment and biota.

Keywords: PFAS; PFOA; SANS; self-assembly; water; urea; denaturation

INTRODUCTION

Surfactants find use in diverse applications on the basis of their ability to adsorb on interfaces and form micelles or lyotropic liquid crystal structures in aqueous solutions. The self-assembly of surfactants in aqueous solutions originates from a balance between the hydrophobic "attraction" resulting from a cavity formation and structuring of water molecules around the surfactant hydrophobe, and the "repulsion" due to electrostatics or hydration between the surfactant head-groups.[1] The presence in water of additives such as polar organic solvents or solutes, electrolytes, and/or ionic liquids can modulate the surfactant self-assembly.[2-8]

Urea is a commonly used additive in aqueous media. Urea is well-known for denaturing proteins[9, 10] and facilitating the dissolution of cellulose[11, 12] on the basis of its ability to modulate hydrophobic interactions.[13-16] Accordingly, the self-assembly of hydrocarbon surfactants in aqueous solution is affected by urea and its derivatives.[17-27] For example, urea increased the critical micelle concentration (CMC) of sodium dodecyl sulfate (SDS) in aqueous solution, and decreased its micelle size and association number.[17, 18, 21] The action of urea in aqueous solutions has been interpreted in terms of a direct mechanism, where urea helps solvate hydrophobic solutes by locating on their solvation layer in the place of water molecules, or an indirect mechanism, whereby urea disrupts the structure of water which, in turn, facilitates the solvation of hydrophobic solutes.[17, 18]

The action of urea on the water network remains controversial, and the structure of urea–water mixtures is not well-understood. Different methods of analysis can lead to different conclusions. Raman,[28] NMR,[29] neutron scattering and some molecular dynamics (MD) simulation studies[10, 30] have indicated that urea acts as a water structure breaker. NMR measurements and Kirkwood–Buff analysis of experimental thermodynamic data of aqueous urea solutions suggest that urea enhances the water structure and acts as a weak water structure maker.[31, 32] Other studies have reported that urea has no effect on the water structure.[33-37] Tera-Hertz absorption spectroscopy,[38] NMR spectroscopy,[33] dielectric spectroscopy,[39] vibrational spectroscopy and other molecular MD simulation studies[40, 41] have indicated that urea has little effect on the water structure, and is neither a structure breaker nor a structure maker. Analysis of water–water radial distribution functions obtained from MD simulations of aqueous urea solution strongly suggested that urea does not disrupt the water structure network.[36] However, the same authors in another publication reported urea to be a water structure breaker based on changes in

the water–water hydrogen bond angle (decrease) and distance (increase).[10] MD simulations of aqueous urea solution using nearest neighbor approach (i.e., only water molecules, and not urea, were considered as neighbors of a reference water molecule) showed urea to induce distortion of the tetrahedral water structure;[42] however, when urea was also considered as a neighbor of the reference water molecule, the MD results showed that urea can substitute for water in the hydrogen-bonded network without breaking the tetrahedral water structure.[37] The disagreement in the case of MD simulations regarding the effect of urea on the water structure network can originate from the different models of urea and water that were used in the simulations, and/or the different choices of statistical properties that were used to quantify the effect.[42]

Compared to the widely used hydrocarbon surfactants, specialty surfactants comprising a fluorocarbon hydrophobic part exhibit unique properties, such as the ability to repel both oil and water, strong surface activity and wetting ability, and high chemical and thermal stability.[3] Hence, fluorinated surfactants have found diverse applications including nonstick cookware, stain repellants, protective coatings, firefighting foams, food packaging, and cosmetics.[43-46] A downside of their chemical and thermal stability is that fluorinated surfactants are very difficult to degrade, resulting in their persistence in the environment (mainly aqueous) and in animal and human bodies, causing adverse heath affects[47-52] and generating concern among the public.

Urea is a major ingredient of agricultural runoff water and urine. As such, urea is likely to affect the behavior of fluorinated surfactants which are present in the aqueous environment and biota. The information published on urea effects on fluorinated surfactants is very limited.[3, 53, 54] Our recent report on the effect of urea on the micellization of the fluorinated surfactant perfluoro-n-octanoic acid ammonium salt (PFOA) supported the direct mechanism of urea action and identified differences between fluorocarbon and hydrocarbon surfactant self-assembly in aqueous urea solutions.[3] While the results presented in that paper provided indirect evidence on urea effects on PFOA micelles, direct structural information on PFOA micelles in aqueous solutions in the presence of urea is not available in the literature. In general, nano-structure characterization studies of fluorinated surfactant micelles in water are limited.[55-61]

With an aim to address this gap in knowledge, we employ here small-angle neutron scattering (SANS) and atomistic molecular dynamics (MD) simulations to obtain direct structural information and understand the molecular organization and interactions in aqueous urea solutions of the representative fluorinated surfactant PFOA. The interactions between

fluorinated surfactants and additives such as urea are important to study since the fundamental knowledge thus gained can be helpful in the design of materials and methods for the removal of fluorinated surfactants from aqueous media or the human body, and in the replacement in certain applications of fluorinated surfactants with environment-friendly alternatives.

EXPERIMENTAL AND THEORETICAL METHODS

Materials

Perfluoro-n-octanoic acid ammonium salt ($C_7F_{15}COONH_4$, CAS number: 3825-26-1, MW = 431.1 g/mol, 98% purity; abbreviated here as PFOA), also known as pentadecafluorooctanoic acid ammonium salt or ammonium perfluorooctanoate, was obtained from SynQuest Laboratories (Alachua, FL, USA) and was used as received. Urea (NH_2CONH_2), 99% pure, was obtained from Alfa Aesar (Haverhill, MA, USA). Deuterium oxide (99.9% D), (D_2O, MW = 20.03 g/mol, 99.5% purity), also known as deuterated water, was obtained from Cambridge Isotope Laboratories, Inc. (Tewksbury, MA, USA) and was used as received. All the samples were prepared using D_2O and were allowed sufficient time to equilibrate following the mixing of ingredients. The PFOA concentration of 110 mM has been selected in the SANS experiments since PFOA micelles are well-defined at this concentration (well above the CMC = 26.5 mM). The urea concentrations selected for study spanned a wide range: 0 – 6 M.

Small-angle neutron scattering (SANS) data collection and reduction

SANS measurements of aqueous PFOA solutions in the absence and in the presence of urea were performed on the NG-7 and NG-B 30 m SANS instruments at the Center for Neutron Research (NCNR), National Institute of Standards and Technology (NIST), Gaithersburg, MD. Neutrons with 6 Å wavelength were focused on samples kept in quartz cells of 2 mm thickness. Sample-to-detector distances (SDD) of 2, 6.5 or 10 m, or 1.33, 4 and 13.17 m were used for each sample in order to cover the wave vector (q) range 0.05 $Å^{-1} < q < 0.5$ $Å^{-1}$. The measurement time was 180 – 3600 seconds. All the raw SANS intensity data were corrected and reduced using the IGOR Pro software. For each sample, reduced SANS data of at three instrument configurations (2, 6.5 or 10 m SDD or 1.33, 4 and 13.17 m SDD) were combined into one data file after trimming data points from the ends of each set and rescaling the overlap regions.[62]

In the data reduction process, scattering intensity raw data were corrected for the scattering from empty cell, background and detector sensitivity, and converted to absolute intensity scale.[62] The scattering contribution from the solvent has been accounted for by fitting a straight line to the solvent intensity data at the high-q range, and subtracting the intensity of this straight line from the sample scattering intensity. The fraction of the solvent scattering intensity subtracted (scale factor f) is the volume fraction of solvent in the sample. The error bars shown

in the various SANS absolute intensity plots were calculated by the IGOR Pro software during the data reduction process. The data points in the low-q region may exhibit relatively large error bars due to scattering from possible air bubbles present in the sample.

SANS data analysis

SANS data from PFOA micelles in D_2O in the absence and in the presence of urea have been fitted with the core-shell ellipsoid form factor and the Hayter – Penfold structure factor with rescaled mean spherical approximation (RMSA).[8]

The overall scattering intensity I(q) is given by:

$$I_{micelle}(q) = A.\phi.P(q).S(q) + B_{inc} \quad (1)$$

P(q) is the form factor representing the shape and structure of a micelle, while S(q) is the structure factor representing the intermicelle interactions in the solution. φ is the volume fraction of the micelles. The parameters A and B_{inc} account for additional contributions due to the absolute scaling and incoherent noise, respectively.

P(q) was calculated using the following equations:

$$P(q) = \frac{scale}{V}F^2(q,\alpha) + background \quad (2)$$

$$F(q,\alpha) = f(q,b,a,\alpha) + f(q,b+\delta,a+\delta.\epsilon,\alpha) \quad (3)$$

where b is the equatorial core radius perpendicular to the rotational axis of the ellipsoid, a is the polar core radius along the rotational axis of the ellipsoid, δ is the thickness of the shell near equator, ϵ is the ratio of shell thickness at pole to that at equator. For a fixed shell thickness ϵ = 1.

$$F\left(q,R_e,R_p,\alpha\right) = \frac{3\Delta\rho V(\sin[qr(R_e,R_p,\alpha)]-\cos[qr(R_e,R_p,\alpha)])}{[qr(R_e,R_p,\alpha)]^3} \quad (4)$$

$$r\left(R_e,R_p,\alpha\right) = [R_e^2 sin^2\alpha + R_p^2 cos^2\alpha]^{1/2} \quad (5)$$

α is the angle between the axis of the ellipsoid and $\vec{q}$, $V = (4/3)\pi R_p R_e^2$ is the volume of the ellipsoid, R_p is the polar radius along the rotational axis of the ellipsoid, R_e is the equatorial radius perpendicular to the rotational axis of the ellipsoid and $\Delta\rho$ (contrast) is the scattering length density difference, either ($\rho_{core} - \rho_{shell}$) or ($\rho_{shell} - \rho_{solvent}$). When the ratio of polar core radius (a) to the equatorial core radius (b) ε (= a/b) < 1 the core is oblate; when ε > 1 it is prolate, and ε = 1 denotes a spherical core.

The structure factor S(q) was calculated using a Hayter−Penfold-type potential,[63] with mean spherical approximation and rescaling corrections for low volume fractions, given the micelle volume fraction, charge on a micelle, and ionic strength of the solution.[8]

Parameters that are adjusted when fitting SANS intensity data with the above described form and structure factors include: scale, background, minor radius of core (b), axial ratio of core (ε), shell thickness at equator (δ), ratio of shell thickness at pole to that at equator (ϵ), shell SLD (ρ_{shell}), core SLD (ρ_{core}), solvent SLD ($\rho_{solvent}$), micelle volume fraction (φ), charge on a micelle (Z), temperature, salt concentration, and dielectric constant of the medium. The micelle association number (η), fractional charge on a micelle (α = Z/η), and the number of urea molecules in close proximity to a micelle (η_{urea}) are other important parameters calculated from the parameters obtained from fitting SANS intensity data. For the fits, we limit the q-range from 0.01 to 0.4 $Å^{-1}$. Table S1 presents values of molecular parameters used for SANS data fittings.

In analyzing the SANS data, we fix the known parameters (e.g., solvent SLD, temperature, ionic strength, dielectric constant of the medium), we make reasonable assumptions for some parameters (e.g., micelle core minor radius (b) equal to the extended length of a PFOA fluorocarbon chain $l_{f,c}$ = 11.14 Å;[3] uniform shell thickness: ratio of shell thickness at pole to that at equator ϵ = 1), and we leave some parameters (e.g., background, volume fraction (φ), charge on a micelle (Z), shell thickness at equator (δ)) free to be adjusted in order to obtain a best fit. The statistical parameter χ_R^2 provided by the software quantifies the differences between the calculated and experimental SANS intensities. χ_R^2 approaches unity for an excellent fit.

For PFOA D_2O solutions we considered the micelle core to consist of only fluorocarbon chains (dry core), and the shell to include carboxylate head-groups, counterions, and associated water molecules. In the case of PFOA in D_2O+urea solutions, the shell contains also some urea.

The major fitting parameters to describe the scattering from PFOA micelles in D_2O and in D_2O+urea are the surfactant association number (η), micelle volume fraction (φ), charge on a micelle (Z), and number of urea molecules per micelle (η_{urea}).

The core volume V_{core} (in $Å^3$) was calculated given the surfactant association number η:

$$V_{core} = \eta V_{t,APFO} \quad (6)$$

where $V_{t,PFOA}$ = 333.6 $Å^3$ is the volume of a PFOA fluorocarbon chain.[3]

The micelle shell volume, considering the hydrophilic head-groups of the surfactant, counterions, urea, and associated water molecules, can be written as:

$$V_{shell} = \eta\left(V_{COO^-} + (1-\alpha)V_{NH_4^+} + N_H V_{D_2O}\right) + \eta_{urea}(V_{urea}) \quad (7)$$

where V_{COO^-} is the volume of the PFOA hydrophilic head-group, $V_{NH_4^+}$ volume of the counterion NH_4^+, V_{D_2O} volume of a D_2O molecule, V_{urea} volume of a urea molecule, N_H hydration number, i.e., number of water molecules associated per surfactant molecule. $\alpha = Z/\eta$ is the fractional charge on a micelle. $V_{urea} = 75.53$ Å^3 was obtained from reference.[64]

An 'ab initio' quantum computational study of PFOA/H_2O system reported that on average 8 water molecules can be accommodated near the polar head-group of the PFO^- ion.[65] The reported hydration numbers for NH_4^+ ion vary widely from 4 to 11.[66, 67] On the basis of the reported hydration numbers for NH_4^+ ion and PFO^- ion, we fixed $N_H = 12$.

The scattering length density of the micelle core is calculated by equation (8)

$$\rho_{core} = \frac{\eta b_{CF_3(CF_2)_6}}{V_{core}} \quad (8)$$

where b_i is the coherent scattering length of molecule i. b_i values reported are shown in Table S1.

The scattering length density of the micelle shell is calculated using equation (9), which includes the individual contributions to the scattering from surfactant hydrophilic head-groups, counterions, urea, and associated water molecules.

$$\rho_{shell} = \frac{\eta\left[b_{COO^-} + (1-\alpha)b_{NH_4^+} + N_H b_{D_2O}\right] + \eta_{urea}[b_{urea}]}{V_{shell}} \quad (9)$$

The scattering length density of the solvent $\rho_{solvent}$ was calculated using the scattering lengths and concentrations of urea, surfactant, and deuterated water. The concentration of PFOA present in the bulk solution was considered as its CMC. The dielectric constant values of aqueous urea solutions are obtained from the literature.[68]

In the case of 110 mM PFOA in D_2O, while fitting SANS intensity data we varied the shell thickness (δ) and calculated the volume of the micelle core (V_{core}) and shell (V_{shell}). From V_{core} and V_{shell}, using equations 6 and 7 ($\eta_{urea} = 0$), we calculated the surfactant association number (η). During the fit, we adjusted the shell thickness such that the association number (η) calculated from V_{core} (equation 6) equals the η value calculated from V_{shell} (equation 7). From η, α, V_{shell} values obtained, we calculated the scattering length density of the shell (ρ_{shell}). In the case of 110 mM PFOA in urea + D_2O, the scattering length density of the shell (ρ_{shell}) depends on η, η_{urea}, α, V_{shell}, (i.e., on ε, δ). The shell thickness (δ) was varied, and η_{urea}, ρ_{shell} were

calculated iteratively such that all the parameters are realistic and the ρ_{shell} value given by software matches with the ρ_{shell} value calculated from equation 9.

The form and structure factor models used in this study for fitting PFOA SANS intensity profiles are consistent with those that have been used by previous SANS studies on fluorinated surfactants.[56, 57] Water-free ("dry") micelle core was previously used in sodium perfluorooctanoate (NaPFO) and cesium perfluorooctanoate (CsPFO) SANS analysis.[56, 57, 59]

Molecular dynamics simulations

Molecular dynamics (MD) simulations were conducted employing a non-polarizable version of the Atomistic Polarizable Potentials for Liquids, Electrolytes and Polymers (APPLE&P) force field.[69] Simulations were conducted at 298 K and surfactant concentrations well above the CMC. Each system contained 32 PFOA molecules and about 4000 water (or water + urea) molecules, which corresponds to 390 mM surfactant concentration (see Supplementary Information (SI) for the exact compositions of all systems). Systems with 0, 1.2, 2.2, and 4 M concentration of urea have been investigated by MD. Initially, all molecules were distributed homogeneously. During equilibration, all 32 PFO^- molecules have self-assembled into one micelle, which is consistent with the selected concentration being much larger than the CMC. Subsequent production simulations showed that the formed micelle is not in a static configuration but underwent extensive fluctuations in shape and dimensions. Moreover, the molecules inside the micelle moved relative to each other and explored the entire micelle as characterized by the analysis of neighboring PFO^- residence times (see SI for details). Since production simulations were much longer than the residence times, we are confident that multiple independent configurations of the micelle were sampled, allowing the converged statistics for the micelle shape and dimensions.

All simulations were run at 298 K, with temperature controlled by the Nose-Hoover thermostat and barostat.[70, 71] The cut-off radius for the van der Waals interactions and electrostatic potential in the real space was set to 15 Å, with a tapering distance of 0.5 Å. The electrostatic interactions in the reciprocal space were calculated using Ewald summation.[72] A multiple time-step technique was applied to enhance the efficiency of integration of the equations of motion. For all bonds and bends, a 0.5 fs time step was used, while a 1.5 fs time step was used for dihedrals and short-range (less than 8.0 Å) non-bonded interactions. For the

remainder of the non-bonded interactions and electrostatic reciprocal space portion, the integration time step was set to 3.0 fs. All bond lengths were constrained with the SHAKE algorithm, with a tolerance of 10^{-14}.[73] Initially, all molecules and ions were placed randomly in a relatively large cubic simulation cell (300 Å in each dimension). Within 300 ps, the simulation cell was shrunk to the dimensions close to the equilibrium size. Subsequent equilibration simulations in the NPT ensemble were conducted in order to establish equilibrium density of the system. Production runs over 30ns were also conducted in the NPT ensemble.

RESULTS AND DISCUSSION

Small-angle neutron scattering analysis

SANS absolute intensity profiles of PFOA solutions in D_2O and in D_2O+urea at 22 °C are shown in Figure 1. The shape of the profiles and the relative intensity can provide qualitative information about structure and interactions. The correlation peak reflects repulsive interactions between the micelles. Upon the addition of urea, the correlation peak shifts to higher-q, indicating a decrease in the intermicelle distance (estimated from the q value at the peak maximum: $d = 2\pi/q_{max}$.). Since the surfactant concentration has been kept constant, such a decrease in d reflects an increase in the micelle number density, which is possible only if the micelles become smaller. The other possibility could have been for less surfactant available to form micelles caused by an increase in CMC; however, this is not the case, since we know that the CMC of PFOA decreases in the presence of 2, 4.4 or 6 M urea.[3] The peak intensity decrease with the addition of urea indicates weaker electrostatic repulsions between the micelles.

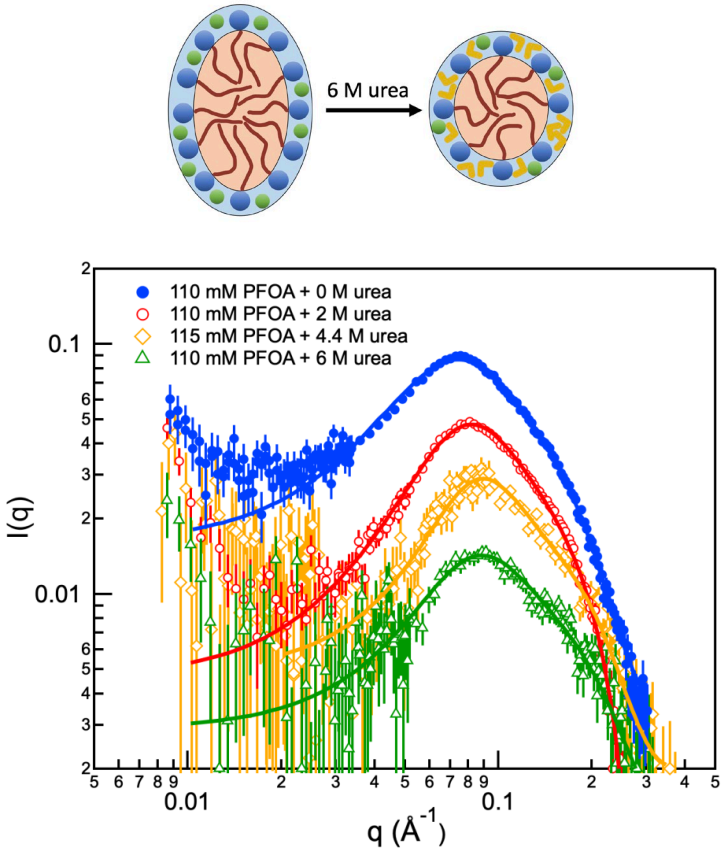

Figure 1. SANS intensity profiles of PFOA in D_2O and in D_2O+urea solutions corrected for solvent scattering. Markers represent experiment data and solid lines represent fits using the core-shell ellipsoid form factor and Hayter RMSA structure factor as described in the text. The schematic shows the effect of urea on the PFOA micelles. The micelles are depicted with a fluorocarbon core and a shell comprising head-groups and water of hydration. Urea molecules localize at the surface of the micelle core, thus directly affecting the PFOA micelle structure.

To obtain quantitative information on the structure and interactions of PFOA micelles in the presence of urea, and on the effect of urea on PFOA micelle structure, the scattering profiles of PFOA in D_2O and in D_2O+urea solutions were fitted using the core-shell ellipsoid form factor and Hayter RMSA structure factor described in the Materials and Methods section. Figure 1 shows the fits (solid lines) and Table 1 summarizes the important parameters obtained by fitting the SANS data for PFOA solutions. Additional parameters are included in SI.

Table 1. Parameters obtained by fitting SANS intensity data of PFOA in D_2O+urea solutions corrected for solvent (D_2O+urea) scattering using the core-shell ellipsoid form factor and the Hayter rescaled MSA structure factor. η association number (i.e., the average number of surfactant molecules per micelle); α fractional charge or charge per surfactant molecule in a micelle; φ volume fraction of the micelles; η_{urea} average number of urea molecules per micelle; v_{urea} %volume of urea in a micelle which comprises PFOA + hydration water + counterions + urea; b micelle core minor radius; ε ratio of micelle core major to minor axis; δ shell thickness; R_{eq} radius of a sphere with volume equal that of the micelle; d inter-micelle distance; and I_{peak} intensity at the correlation peak maximum. χ_R^2 is a statistical parameter that quantifies the differences between the calculated and experimental SANS data set. The uncertainties in the major parameters (shown in parenthesis) are calculated by applying propagation of errors using statistical uncertainties of the fitting parameters.

PFOA (mM)	Urea (M)	η	α	ε	b (Å)	δ (Å)	R_{eq} (Å)
110	0	30 (±0.2)	0.27 (±0.004)	1.73 (±0.007)	11.14	4.12	17.6 (±0.02)
110	2	23 (±0.3)	0.46 (±0.008)	1.30 (±0.005)	11.14	4.10	16.3 (±0.02)
115	4.4	21 (±0.3)	0.61 (±0.043)	1.20 (±0.017)	11.14	4.24	16.1 (±0.06)

110	6	19.5 (±0.5)	0.52 (±0.044)	1.12 (±0.024)	11.14	4.40	16.0 (±0.08)
PFOA (mM)	Urea (M)	η_{urea}	v_{urea}	Φ x 10^3	d (Å)	I_{peak}	χ_R^2
110	0	0	0	24.5 (±0.1)	84.9	0.088	2.48
110	2	13.9 (±0.7)	5.8 (±0.3)	25.4 (±0.1)	76.6	0.048	1.91
115	4.4	23.7 (±2.1)	10.2 (±0.9)	32.4 (±0.7)	69.8	0.029	1.25
110	6	32.1 (±2.9)	14.1 (±1.3)	29.8 (±0.9)	70.6	0.014	1.20

The effects of added urea on PFOA micelle characteristics are depicted in Figure 2. The decrease in the CMC of PFOA with urea addition can be ascribed to the combined effect of urea on electrostatic and hydrophobic interactions.[3] Added urea has two mechanisms affecting electrostatic interactions in the system: (a) the increase of dielectric constant of the solution with addition of urea decreases the electrostatic attraction between COO^- head-group and NH_4^+counterion, and also the repulsion between COO^- head-groups, thus favoring micellization; (b) direct strong electrostatic interaction between urea and COO^- head-group replaces water from the interface with micelle. The urea effects on electrostatics are reflected in the increase (doubling) in the fractional charge on a micelle, α, i.e., degree of counterion dissociation. Addition of 2, 4.4 or 6 M urea increased the fractional charge on a micelle, α, by 70, 126 and 93 %, respectively, due to a decrease in the attraction between head-group COO^- and counterion NH_4^+ and in the head-group–head-group repulsions. In addition, the urea molecules strongly interacting with head-groups on the micelle surface have to also interact with neighboring fluorocarbons. Urea–fluorocarbon interactions decrease the hydrophobic effect thus opposing micellization. Given that the CMC decreases, it appears that the effect of urea on the electrostatics is stronger that its effect on the hydrophobic interactions.

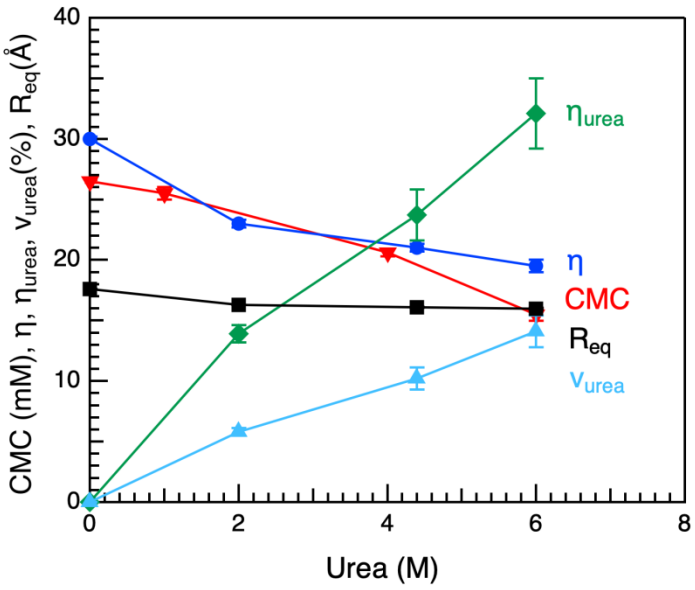

Figure 2. CMC (in mM), association number (η), average number of urea molecules per micelle (η_{urea}), volume percent of urea (v_{urea}) in a micelle which comprises [PFOA + hydration water + counterions + urea], and radius (in Å) of a sphere with volume equal that of the micelle (R_{eq}), plotted as a function of urea concentration in the aqueous solution (the lines are guides to the eye). The CMC values plotted are taken from reference.[3]

The addition of 2, 4.4 or 6 M urea to aqueous PFOA solutions resulted in a decrease in the association number by 24, 30 and 35 %, respectively, relative to the zero urea case. The number of urea molecules per micelle also increased with the added urea concentration. Urea localization in the PFOA micelle shell should increase the average area per PFOA head-group at the micelle surface. Indeed, dividing the surface area of the micelle by the association number results in 134 Å^2 per surfactant head-group at 0 M urea and 165 Å^2 per head-group at 6 M urea. Surface tension results also show an increase in the surface area per head-group of PFOA micelles with urea addition.[3] The PFOA micelle volume decreased by 20-25% and the radius of a sphere with volume equal that of the micelle (R_{eq}) decreased by about 10% with the addition of 2-6 M urea. The SANS results also show the micelle shape to change with urea addition from prolate ellipsoid to sphere: the ratio of micelle core major to minor axis (ε) decreased from 1.73 at 0 M urea to 1.12 at 6 M urea. Such a micelle shape change due to urea addition was previously inferred from critical packing parameter (CCP) values.[3]

These effects of urea on the PFOA micellization are consistent with the direct mechanism of urea action, whereby urea localizes at the micelle surface (shell) by replacing some water molecules, increases the surface area per PFOA head-group, decreases the surfactant packing density at the micelle surface and, correspondingly, affects the micelle size and shape.

SANS studies on fluorinated surfactant micelles in aqueous solutions in the presence of additives are very limited. A few SANS studies are available on mixed micelles of fluorinated surfactants and hydrogenated surfactants[59, 74-76] or imidazolium-based ionic liquids,[60] and on PFOA micelles in the presence of salt:[55, 61] in NH_4Cl: NH_4OH buffer solutions with pH 8.8 and an ionic strength of 0.1 (units not mentioned in that paper), and in 0.5 M NH_4Cl.

Urea effects on the hydrocarbon surfactant SDS have not been studied by SANS, to the best of our knowledge. SANS studies on urea effects on gemini surfactants of the ethanediyl- α-ω-bis(alkyldimethylammonium bromide) type, referred to as ‘‘m-2-m” (m = 12, 14 and 16) i.e. (12-2-12, 14-2-14, 16-2-16) and polyoxyethylene surfactants are available.[25, 26] The direct mechanism of urea action has been reported for the gemini surfactants.[25] The SANS results have shown that the 12-2-12 gemini surfactant forms prolate ellipsoid micelles and, with an increase in the added urea concentration, the scattering cross-section decreases and the correlation peak shifts to higher q values, indicating a decrease in the size of micelles.[25] The same type of behavior was observed in the PFOA SANS profiles reported here. It has also been observed that the length of semi-major axis and the association number of the 12-2-12 micelles decrease with increase in urea concentration, which agrees well with our SANS results for PFOA.[25] In the case of polyoxyethylene surfactants, the presence of urea increased the CMC, and SANS results have shown that, for surfactants with a high ratio of head-group size to tail length (n-dodecylhexaoxyethylene ($C_{12}E_6$) and n-octylytetraoxyethylene (C_8E_4)), the micelles transitioned from elongated to globular.[26] Whereas, surfactants that form globular micelles in the absence of urea preserve this shape as the urea concentration is increased (n-octylpentaoxyethylene (C_8E_5) and n-dodecyloctaoxylethylene ($C_{12}E_8$)).[26]

Molecular dynamics simulations analysis

To obtain additional, molecular-scale insights, atomistic MD simulations have been conducted on PFOA aqueous solutions with different concentrations of urea. The influence of urea concentration on the micelle structure can be seen in Figure 3, in which a compact packing

of the micelle is observed for all concentrations of urea tested, ranging from 0 M to 4.0 M. In water (no urea present), about 39% of ammonium counterions are dissociated from the PFO^- surfactant, which is in a good agreement with experimental data. In pure water, the micelle comprised of 32 PFOA chains has slightly ellipsoidal (prolate) shape with the average principal moments of squared radius of gyration being R_{11}^2 =62.9 Å^2, R_{22}^2 =43.5 Å^2, R_{33}^2 =31.3 Å^2, showing that one dimension is noticeably larger (by about 20-40%) than the other two dimensions. With an increase of the urea concentration, the shape of the micelle becomes less asymmetric, i.e., more spherical, with the principal moments of squared radius of gyration being R_{11}^2 =57.2 Å^2, R_{22}^2 =44.1 Å^2, R_{33}^2 =30.9 Å^2, a shape change which is consistent with the results of SANS data analysis. Note that, on the time scale of our simulations in systems containing less than 4.0 M urea, we still observe only one micelle comprised of all 32 PFO^- molecules. However, at the highest urea concentration 4.0 M we observe a single PFOA molecule that is not part of the micelle. This suggests that micelles with smaller association numbers are more stable upon addition of urea, which is consistent with the decrease in η observed in SANS experiments.

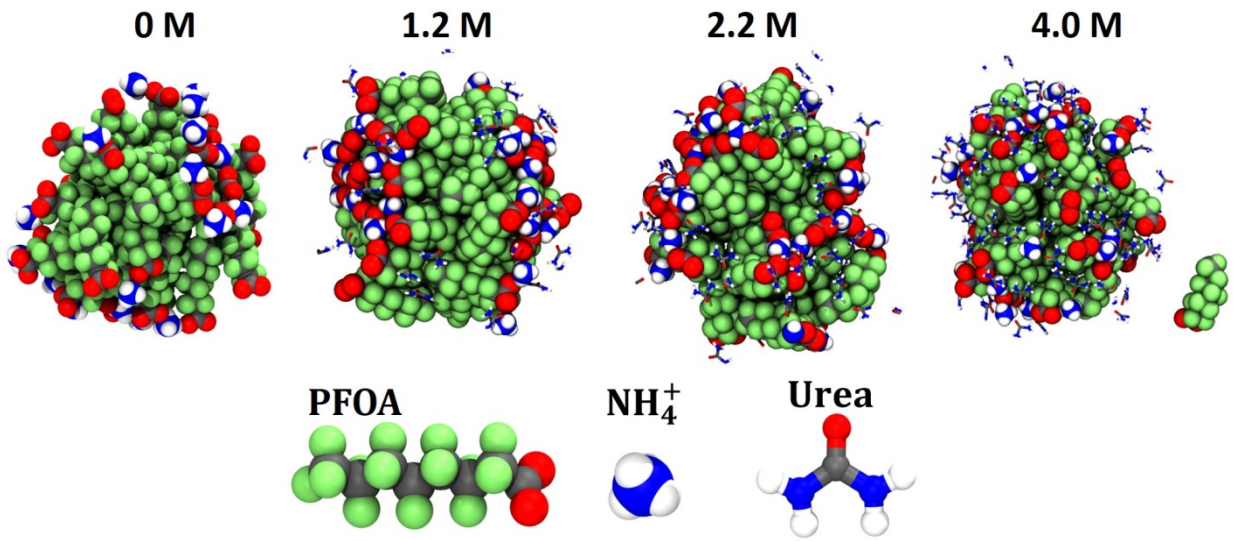

Figure 3. Morphologies of PFOA micelles at different urea concentrations.

To better understand the role of urea and its interaction with the PFOA micelle, the number density of urea molecules, and structural correlations between carbon atom of urea (C) and PFO^- atoms (oxygen O_{COO} and fluorine F) were analyzed and are shown in Figure 4a and 4b,

respectively. For all concentrations, urea molecules are located in the water phase or on the surface of the micelle, without penetrating into the micelle interior. This can be clearly seen from Figure 4a that shows no probability of finding urea molecules in the micelle core. The peaks in the urea density profiles are located at the same distance with respect to the center of micelle, indicating that the radius of micelle does not change much when changing the urea concentration. The radial distribution functions (RDF) and apparent coordination numbers (CN) between urea C atom and O_{COO} or F atoms of PFO^- can be found in Figure 4b. For C_{urea}-O_{COO} RDF, a well-defined peak can be identified at 4.0 Å, indicating strong binding between COO^- head-groups and urea molecules. On average, each COO^- head-group has about 1.5 urea molecules in its first coordination shell (within 5 Å). While the C_{urea}-F RDF is below 1.0 up to separations of 11 Å, the coordination numbers indicate plenty of interaction between urea molecules and F exposed to the surface of the micelle. Figure 4c shows the number of urea and water molecules that are within 5 Å from F atoms, i.e., in contact with exposed F atoms on the micelle surface. With increase of urea concentration, the number of urea molecules in contact with F atoms is increasing linearly, while the number of water molecules drops from about 270 per micelle to 220 at 1.2 M, and to 180 at 4.0 M urea solutions. This confirms the above discussed interpretation of SANS data that suggested a replacement of interfacial water with urea.

MD simulations have shown that urea molecules do not penetrate into the micelle interior but are localized on the surface of the micelles. This is consistent with the micelle composition scenario that we considered while fitting the SANS data, in which urea molecules are present in the micelle shell and not in the micelle core. The location of the peaks observed at around 15 Å in the urea density profiles (Fig. 4a) for different urea concentrations matches well with the micelle radius R_{eq} values (~16 Å) obtained from SANS. Therefore, both SANS and MD simulations indicate that there is no big change in the radius of micelles when changing the urea concentration. Coming to the number of urea molecules per PFOA in a micelle, MD simulations show 1.5 urea molecules per each COO^- head-group in the first coordination shell at 4.0 M urea, which is in good agreement with the 1.1 urea molecules, on average, per PFOA molecule in the micelle that has been obtained from SANS analysis at 4.4 M urea.

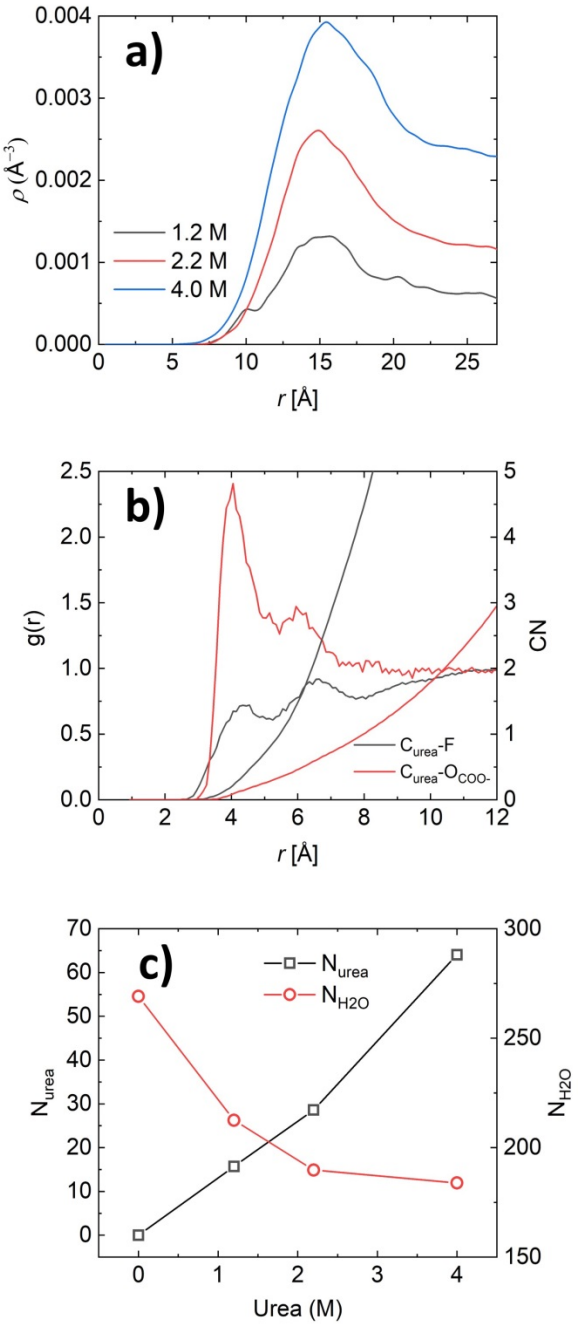

Figure 4. a) Number density of urea molecules with respect to the center of mass of PFOA micelle, b) radial distribution functions, g(r), and coordination numbers, CN, between the C atom of urea and oxygen (O_{COO}) and fluorine (F) atoms of PFOA at 4.0 M urea solution, c) number of water and urea molecules that are in contact with F atoms, i.e., interacting with hydrophobic sections of micellar surface, as a function of urea concentration.

CONCLUSIONS

This study concludes on the molecular-level structure of fluorinated surfactant micelles in aqueous solution, focusing on understanding the effects of the additive urea on the molecular organization and interactions, as revealed by analysis of SANS experiments and atomistic MD simulations.

Complementary evidence is obtained for the direct mechanism of urea action on PFOA micellization: Urea helps solvate the hydrophobic micelle core by localizing at the surface of the core in the place of some water molecules. Several -CF_2- groups are exposed to water at the shell of the micelle, and the presence of urea adjacent to these -CF_2- groups is preferable to that of water. SANS experiments and MD simulations agree with the localization of urea on the surface (shell) of the micelles. MD simulations have shown that urea molecules do not penetrate into the micelle interior. The large dipole moment of urea molecules, and their ability to have strong electrostatic interactions with PFO^- head-groups, make these molecules stay preferentially in the aqueous environment rather than partition into the hydrophobic and non-polar core of the micelle. At the same time, urea molecules can efficiently replace water molecules on the micellar surface and minimize the hydrophobic interactions.

The fractional charge on a micelle, α, increases by 70, 126 and 93 %, with the addition of 2, 4.4 or 6 M urea, respectively, which is related to a decrease in the attraction between head-group COO^- and counterion NH_4^+ and in headgroup–headgroup repulsions. The number of urea molecules localized on the micelle shell increase with the concentration of added urea. The ratio of urea molecules preferentially located in the micelle shell to the number of surfactant molecules comprising the micelle (η_{urea}/η) is 0.6, 1.1, and 1.6, at 2, 4.4, and 6 M urea, respectively, from SANS analysis. A similar trend is observed from MD simulations, where an almost linear increase of urea molecules in the micellar shell is observed with an increase of urea concentration. The decrease in the headgroup–headgroup repulsions and headgroup–counterion attractions, and the localization of urea molecules at the micelle surface increases the surface area per PFOA head-group (from 134 $Å^2$ at 0 M urea to 165 $Å^2$ at 6 M urea) and decreases the PFOA packing density at the micelle surface. This causes a change in the micelle shape from prolate ellipsoid to sphere, as evident from the decrease in the ratio of the micelle major to minor core axis (ε) from 1.7 at 0 M urea to 1.1 at 6 M urea.

The micelle association number decreases by 24, 30 and 35 % with the addition of 2, 4.4 or 6 M urea, respectively. Urea stabilizes smaller micelles on the basis of (i) decreased electrostatic interactions and head-group packing density at the micelle surface where urea is located, and (ii) decreased hydrophobic effect due to urea–fluorocarbon interactions. Whereas on the MD simulation time scale we cannot access micelle formation/breaking kinetics, the simulations primarily observe a single micelle comprised of 32 PFOA molecules. However at higher urea compositions, the simulation show separation of one PFOA molecule from the micelle, indicating that smaller micelle sizes are more thermodynamically stable at these conditions. The addition of urea to aqueous PFOA solutions decreases the micelle size as evidenced by the decrease in the micelle volume by 20, 23 and 25%, and radius by 7.5, 8.5 and 9%, with the addition of 2, 4.4 or 6 M urea, respectively. The micelle radius and volume decrease to a smaller extent than the association number due to the localization at the micelle of urea molecules which add to the micelle size (v_{urea} = 5.8, 10.2, 14.1 vol%). Both SANS and MD simulations indicate that there is no big change in the radius of micelles when changing urea concentration.

This is the first study to provide direct structural evidence on the effect of urea on micelles assembled by fluorinated surfactant. Also the first SANS study and first MD simulation study on fluorinated surfactants in the presence of urea. Furthermore, it is one of very few SANS or MD studies available on urea effects on surfactant micelles. The results presented in this study provide fundamental information which might benefit the removal of fluorinated surfactants from the aqueous environment, and the reformulation of fluorinated surfactant-containing products still used in various applications.

Acknowledgements: This research was funded by the U.S. National Science Foundation (NSF), grant numbers CBET-1930959 and CBET-1930935. The generous allocation and technical support from the Center for High Performance of Computing at the University of Utah are gratefully acknowledged. We acknowledge the support of the National Institute of Standards and Technology (NIST), U.S. Department of Commerce, in providing the neutron research facilities used in this work. Access to the CHRNS 30m small-angle neutron scattering instrument was provided by the Center for High Resolution Neutron Scattering (CHRNS), a partnership between NIST and NSF under Agreement No. DMR-1508249. We thank Dr. Yimin Mao at NIST for

valuable assistance with the SANS data acquisition. We thank Emmanuel Nsengiyumva and Ruksana Jahan for help with SANS experiments. SK acknowledges funding from the Mark Diamond Research Fund (MDRF) of the Graduate Student Association at the University at Buffalo, State University of New York (SUNY).

Supporting Information Description: SANS scattering lengths and parameters; force field parameters used in MD simulations; force field verification of urea molecules in water.

REFERENCES

1. Kronberg, B.; Holmberg, K.; Lindman, B., Two fundamental forces in surface and colloid chemistry. In *Surface Chemistry of Surfactants and Polymers*, John Wiley & Sons, Incorporated: Somerset, 2014; pp 65-74.
2. He, Z.; Ma, Y.; Alexandridis, P., Comparison of ionic liquid and salt effects on the thermodynamics of amphiphile micellization in water. *Colloids and Surfaces A: Physicochemical and Engineering Aspects* **2018,** *559*, 159-168.
3. Kancharla, S.; Canales, E.; Alexandridis, P., Perfluorooctanoate in Aqueous Urea Solutions: Micelle Formation, Structure, and Microenvironment. *International Journal of Molecular Sciences* **2019,** *20* (22), 5761.
4. Alexandridis, P.; Holzwarth, J. F., Differential Scanning Calorimetry Investigation of the Effect of Salts on Aqueous Solution Properties of an Amphiphilic Block Copolymer (Poloxamer). *Langmuir* **1997,** *13* (23), 6074-6082.
5. Yang, L.; Alexandridis, P., Polyoxyalkylene Block Copolymers in Formamide−Water Mixed Solvents: Micelle Formation and Structure Studied by Small-Angle Neutron Scattering. *Langmuir* **2000,** *16* (11), 4819-4829.
6. Sarkar, B.; Lam, S.; Alexandridis, P., Micellization of alkyl-propoxy-ethoxylate surfactants in water-polar organic solvent mixtures. *Langmuir* **2010,** *26* (13), 10532-10540.
7. Kancharla, S.; Zoyhofski, N. A.; Bufalini, L.; Chatelais, B. F.; Alexandridis, P., Association between Nonionic Amphiphilic Polymer and Ionic Surfactant in Aqueous Solutions: Effect of Polymer Hydrophobicity and Micellization. *Polymers* **2020,** *12* (8), 1831.
8. Fajalia, A. I.; Tsianou, M., Charging and uncharging a neutral polymer in solution: A small-angle neutron scattering investigation. *Journal of Physical Chemistry B* **2014,** *118* (36), 10725-10739.
9. Wallqvist, A.; Covell, D. G.; Thirumalai, D., Hydrophobic Interactions in Aqueous Urea Solutions with Implications for the Mechanism of Protein Denaturation. *Journal of American Chemical Society* **1998,** *120* (2), 427-428.
10. Das, A.; Mukhopadhyay, C., Urea-Mediated Protein Denaturation: A Consensus View. *Journal of Physical Chemistry B* **2009,** *113* (38), 12816-12824.
11. Alexandridis, P.; Ghasemi, M.; Furlani, E. P.; Tsianou, M., Solvent processing of cellulose for effective bioresource utilization. *Current Opinion in Green and Sustainable Chemistry* **2018,** *14*, 40-52.
12. Alves, L.; Medronho, B.; Filipe, A.; E Antunes, F.; Lindman, B.; Topgaard, D.; Davidovich, I.; Talmon, Y., New Insights on the Role of Urea on the Dissolution and Thermally-Induced Gelation of Cellulose in Aqueous Alkali. *Gels* **2018,** *4* (4), 87.
13. Priya, M. H.; Ashbaugh, H. S.; Paulaitis, M. E., Cosolvent Preferential Molecular Interactions in Aqueous Solutions. *Journal of Physical Chemistry B* **2011,** *115* (46), 13633-13642.
14. Trzesniak, D.; van der Vegt, N. F. A.; van Gunsteren, W. F., Computer simulation studies on the solvation of aliphatic hydrocarbons in 6.9 M aqueous urea solution. *Physical Chemistry Chemical Physics* **2004,** *6* (4), 697-702.
15. Graziano, G., On the Solubility of Aliphatic Hydrocarbons in 7 M Aqueous Urea. *Journal of Physical Chemistry B* **2001,** *105* (13), 2632-2637.
16. Ikeguchi, M.; Nakamura, S.; Shimizu, K., Molecular dynamics study on hydrophobic effects in aqueous urea solutions. *Journal of American Chemical Society* **2001,** *123* (4), 677-682.

17. Ruiz, C. C., A photophysical study of the urea effect on micellar properties of sodium dodecylsulfate aqueous solutions. *Colloid and Polymer Science* **1995,** *273* (11), 1033-1040.
18. Baglioni, P.; Rivara-Minten, E.; Dei, L.; Ferroni, E., ESR study of sodium dodecyl sulfate and dodecyltrimethylammonium bromide micellar solutions. Effect of urea. *Journal of Physical Chemistry* **1990,** *94* (21), 8218-8222.
19. Briganti, G.; Puvvada, S.; Blankschtein, D., Effect of urea on micellar properties of aqueous solutions of nonionic surfactants. *Journal of Physical Chemistry* **1991,** *95* (22), 8989-8995.
20. Kumar, S.; Parveen, N.; Kabir ud, D., Effect of urea addition on micellization and the related phenomena. *Journal of Physical Chemistry B* **2004,** *108* (28), 9588-9592.
21. Abuin, E. B.; Lissi, E. A.; Aspée, A.; Gonzalez, F. D.; Varas, J. M., Fluorescence of 8-Anilinonaphthalene-1-sulfonate and Properties of Sodium Dodecyl Sulfate Micelles in Water–Urea Mixtures. *Journal of Colloid and Interface Science* **1997,** *186* (2), 332-338.
22. Almgren, M.; Swarup, S., Size of sodium dodecyl sulfate micelles in the presence of additives i. alcohols and other polar compounds. *Journal of Colloid and Interface Science* **1983,** *91* (1), 256-266.
23. De Moura, A. F.; Bernardino, K.; De Oliveira, O. V.; Freitas, L. C. G., Solvation of sodium octanoate micelles in concentrated urea solution studied by means of molecular dynamics simulations. *Journal of Physical Chemistry B* **2011,** *115* (49), 14582-14590.
24. Alexandridis, P.; Athanassiou, V.; Hatton, T. A., Pluronic-P105 PEO-PPO-PEO Block Copolymer in Aqueous Urea Solutions: Micelle Formation, Structure, and Microenvironment. *Langmuir* **1995,** *11* (7), 2442-2450.
25. Mahajan, R. K.; Kaur, R.; Aswal, V. K., Effect of urea on the aggregation behavior of gemini surfactants and their mixed micelles with Pluronic L64. *Colloids and Surfaces A: Physicochemical and Engineering Aspects* **2013,** *419*, 61-68.
26. Bianco, C. L.; Schneider, C. S.; Santonicola, M.; Lenhoff, A. M.; Kaler, E. W., Effects of urea on the microstructure and phase behavior of aqueous solutions of polyoxyethylene surfactants. *Industrial & Engineering Chemistry Research* **2010,** *50* (1), 85-96.
27. Espinosa, Y. R.; Grigera, R. J.; Ferrara, C. G., Mechanisms associated with the effects of urea on the micellar structure of sodium dodecyl sulphate in aqueous solutions. *Progress in Biophysics and Molecular Biology* **2018,** *140*, 117-123.
28. Walrafen, G. E., Raman Spectral Studies of the Effects of Urea and Sucrose on Water Structure. *Journal of Chemical Physics* **1966,** *44* (10), 3726.
29. Sacco, A.; Holz, M., NMR studies on hydrophobic interactions in solution Part 2.—Temperature and urea effect on the self-association of ethanol in water. *Journal of the Chemical Society, Faraday Transactions* **1997,** *93* (6), 1101-1104.
30. Soper, A. K.; Castner, E. W.; Luzar, A., Impact of urea on water structure: a clue to its properties as a denaturant? *Biophysical Chemistry* **2003,** *105* (2), 649-666.
31. Chitra, R.; Smith, P. E., Molecular Association in Solution: A Kirkwood−Buff Analysis of Sodium Chloride, Ammonium Sulfate, Guanidinium Chloride, Urea, and 2,2,2-Trifluoroethanol in Water. *Journal of Physical Chemistry B* **2002,** *106* (6), 1491-1500.
32. Mayele, M.; Holz, M., NMR studies on hydrophobic interactions in solution Part 5. Effect of urea on the hydrophobic self-association of tert-butanol in water at different temperatures. *Physical Chemistry Chemical Physics* **2000,** *2* (10), 2429-2434.

33. Shimizu, A.; Fumino, K.; Yukiyasu, K.; Taniguchi, Y., NMR studies on dynamic behavior of water molecule in aqueous denaturant solutions at 25 °C: Effects of guanidine hydrochloride, urea and alkylated ureas. *Journal of Molecular Liquids* **2000,** *85* (3), 269-278.
34. Hua, L.; Zhou, R.; Thirumalai, D.; Berne, B. J., Urea Denaturation by Stronger Dispersion Interactions with Proteins than Water Implies a 2-Stage Unfolding. *Proceedings of the National Academy of Sciences of the United States of America* **2008,** *105* (44), 16928-16933.
35. Kokubo, H.; Pettitt, B. M., Preferential solvation in urea solutions at different concentrations: properties from simulation studies. *Journal of Physical Chemistry B* **2007,** *111* (19), 5233-5242.
36. Das, A.; Mukhopadhyay, C., Atomistic mechanism of protein denaturation by urea. *Journal of Physical Chemistry B* **2008,** *112* (26), 7903-7908.
37. Bandyopadhyay, D.; Mohan, S.; Ghosh, S. K.; Choudhury, N., Molecular dynamics simulation of aqueous urea solution: is urea a structure breaker? *Journal of Physical Chemistry B* **2014,** *118* (40), 11757-11768.
38. Funkner, S.; Havenith, M.; Schwaab, G., Urea, a structure breaker? Answers from THz absorption spectroscopy. *Journal of Physical Chemistry B* **2012,** *116* (45), 13374-13380.
39. Hayashi, Y.; Katsumoto, Y.; Omori, S.; Kishii, N.; Yasuda, A., Liquid structure of the urea-water system studied by dielectric spectroscopy. *Journal of Physical Chemistry B* **2007,** *111* (5), 1076-1080.
40. Carr, J. K.; Buchanan, L. E.; Schmidt, J. R.; Zanni, M. T.; Skinner, J. L., Structure and dynamics of urea/water mixtures investigated by vibrational spectroscopy and molecular dynamics simulation. *Journal of Physical Chemistry B* **2013,** *117* (42), 13291-13300.
41. Kuharski, R. A.; Rossky, P. J., Molecular dynamics study of solvation in urea water solution. *Journal of the American Chemical Society* **1984,** *106* (20), 5786-5793.
42. Idrissi, A.; Gerard, M.; Damay, P.; Kiselev, M.; Puhovsky, Y.; Cinar, E.; Lagant, P.; Vergoten, G., The effect of urea on the structure of water: a molecular dynamics simulation. *Journal of Physical Chemistry B* **2010,** *114* (13), 4731-4738.
43. Kissa, E., *Fluorinated Surfactants and Repellents, 2nd Edition*. Marcel Dekker, Incorporated: New York, 2001; Vol. 97, p 1-615.
44. Krafft, M. P., Fluorocarbons and fluorinated amphiphiles in drug delivery and biomedical research. *Advanced Drug Delivery Reviews* **2001,** *47* (2), 209-228.
45. Renner, R., The long and the short of perfluorinated replacements. *Environmental Science & Technology* **2006,** *40* (1), 12-13.
46. Kissa, E., *Fluorinated Surfactants: Synthesis, Properties, Applications*. Marcel Dekker, Incorporated: New York, 1994; Vol. 50.
47. Xiao, F., Emerging poly- and perfluoroalkyl substances in the aquatic environment: A review of current literature. *Water Research* **2017,** *124*, 482-495.
48. Wang, Z. Y.; DeWitt, J. C.; Higgins, C. P.; Cousins, I. T., A Never-Ending Story of Per- and Polyfluoroalkyl Substances (PFASs)? *Environmental Science & Technology* **2017,** *51* (5), 2508-2518.
49. Chang, E. T.; Adami, H.-O.; Boffetta, P.; Cole, P.; Starr, T. B.; Mandel, J. S., A critical review of perfluorooctanoate and perfluorooctanesulfonate exposure and cancer risk in humans. *Critical Reviews in Toxicology* **2014,** *44* (sup1), 1-81.
50. Mohamed, A.; Amith, M.; Nishanth, T.; Tanju, K., The overlooked short- and ultrashort-chain poly- and perfluorinated substances: A review. *Chemosphere* **2019,** *220*, 866-882.

51. United States Environmental Protection Agency (U.S. EPA). 2019. EPA's per- and polyfluoroalkyl substances (PFAS) action plan, EPA 823R18004. https://www.epa.gov/sites/production/files/2019-02/documents/pfas_action_plan_021319_508compliant_1.pdf [accessed March 2021].
52. Alves, A. V.; Tsianou, M.; Alexandridis, P., Fluorinated Surfactant Adsorption on Mineral Surfaces: Implications for PFAS Fate and Transport in the Environment. *Surfaces* **2020,** *3* (4), 516-566.
53. Asakawa, T.; Hashikawa, M.; Amada, K.; Miyagishi, S., Effect of urea on micelle formation of fluorocarbon surfactants. *Langmuir* **1995,** *11* (7), 2376-2379.
54. Zhou, H. T.; Xing, H.; Wu, B. W.; Cao, A. Q.; Xiao, J. X., Hydrotrope-Induced Enhancement of Room Temperature Surface Activity for High Krafft Point Fluorinated Surfactants. *Journal of Surfactants and Detergents* **2016,** *19* (6), 1199-1207.
55. Burkitt, S. J.; Ottewill, R. H.; Hayter, J. B.; Ingram, B. T., Small angle neutron scattering studies on micellar systems part 1. Ammonium octanoate, ammonium decanoate and ammonium perfluoroocatanoate. *Colloid & Polymer Science* **1987,** *265* (7), 619-627.
56. Berr, S. S.; Jones, R. R. M., Small-angle neutron scattering from aqueous solutions of sodium perfluorooctanoate above the critical micelle concentration. *Journal of Physical Chemistry* **1989,** *93* (6), 2555-2558.
57. Iijima, H.; Kato, T.; Yoshida, H.; Imai, M., Small-angle X-ray and neutron scattering from dilute solutions of cesium perfluorooctanoate. Micellar growth along two dimensions. *Journal of Physical Chemistry B* **1998,** *102* (6), 990-995.
58. Downer, A.; Eastoe, J.; Pitt, A. R.; Penfold, J.; Heenan, R. K., Adsorption and micellisation of partially- and fully-fluorinated surfactants. *Colloids and Surfaces A: Physicochemical and Engineering Aspects* **1999,** *156* (1), 33-48.
59. Caponetti, E.; Martino, D. C.; Martino, D. C.; Floriano, M. A.; Triolo, R., Fluorinated, protonated, and mixed surfactant solutions: A small-angle neutron scattering study. *Langmuir* **1993,** *9* (5), 1193-1200.
60. Padsala, S.; Patel, V. I.; Ray, D.; Aswal, V. K.; Bahadur, P., Mixed micelles of sodium perfluorooctanoate and imidazolium based ionic liquids in aqueous solution: A SANS and Tensiometric study. *Journal of Molecular Liquids* **2020**, *322*, 114558.
61. Kunze, B.; Kalus, J.; Boden, N.; Brandao, M. S. B., Transition from rod- to disk-like micelles in APFO/D_2O/NH_4Cl systems studied by SANS and SAXS. *Physica B: Condensed Matter* **1997,** *234*, 351-352.
62. Kline, S. R., Reduction and analysis of SANS and USANS data using IGOR Pro. *Journal of Applied Crystallography* **2006,** *39* (6), 895-900.
63. Hayter, J. B.; Penfold, J., An analytic structure factor for macroion solutions. *Molecular Physics* **1981,** *42* (1), 109-118.
64. Jakli, G.; Van Hook, W. A., Isotope effects in aqueous systems. 12. Thermodynamics of urea-h4/water and urea-d4/water-d2 solutions. *Journal of Physical Chemistry* **1981,** *85* (23), 3480-3493.
65. Duvoisin, S.; Kuhnen, C. A.; Ouriques, G. R., Theoretical study of the ammonium perfluorooctanoate/water system. *Journal of Molecular Structure: Theochem* **2002,** *617* (1), 201-207.
66. Ohtaki, H.; Radnai, T., Structure and dynamics of hydrated ions. *Chemical Reviews* **1993,** *93* (3), 1157-1204.

67. Singh, G.; Verma, R.; Wagle, S.; Gadre, S. R., Explicit hydration of ammonium ion by correlated methods employing molecular tailoring approach. *Molecular Physics* **2017,** *115* (21-22), 2708-2720.
68. Wyman, J., Dielectric Constants: Ethanol—Diethyl Ether and Urea—Water Solutions between 0 and 50. *Journal of the American Chemical Society* **1933,** *55* (10), 4116-4121.
69. Borodin, O., Polarizable Force Field Development and Molecular Dynamics Simulations of Ionic Liquids. *Journal of Physical Chemistry B* **2009,** *113* (33), 11463-11478.
70. Evans, D. J.; Lee Holian, B., The Nose-Hoover thermostat. *Journal of Chemical Physics* **1985,** *83* (8), 4069-4074.
71. Hoover, W. G., Canonical dynamics: equilibrium phase-space distributions. *Physical Review A* **1985,** *31* (3), 1695-1697.
72. Yeh, I. C.; Berkowitz, M. L., Ewald summation for systems with slab geometry. *Journal of Chemical Physics* **1999,** *111* (7), 3155-3162.
73. Palmer, B. J., Direct Application of Shake to the Velocity Verlet Algorithm. *Journal of Computational Physics* **1993,** *104* (2), 470-472.
74. Pedone, L.; Martino, D. C.; Caponetti, E.; Floriano, M. A.; Triolo, R., Determination of the composition of mixed hydrogenated and fluorinated micelles by small angle neutron scattering. *Journal of Physical Chemistry B* **1997,** *101* (46), 9525-9531.
75. Almgren, M.; Garamus, V. M.; Nordstierna, L.; Luc-Blin, J.; Stébé, M.-J., Nonideal mixed micelles of fluorinated and hydrogenous surfactants in aqueous solution. NMR and SANS studies of anionic and nonionic systems. *Langmuir* **2010,** *26* (8), 5355.
76. Burkitt, S. J.; Ottewill, R. H.; Hayter, J. B.; Ingram, B. T., Small angle neutron scattering studies on micellar systems part 2. Mixed systems of ammonium decanoate and ammonium perfluoro-octanoate. *Colloid & Polymer Science* **1987,** *265* (7), 628-636.

Structure and Interactions in Perfluorooctanoate Micellar Solutions Revealed by Small-Angle Neutron Scattering and Molecular Dynamics Simulations Studies: Effect of Urea

Table of Contents Image